International Journal of Engineering & Technology, 8 (1.2) (2019) 153-156

International Journal of Engineering & Technology

Website: www.sciencepubco.com/index.php/IJET

Research paper



Structural and Morphological Characterization of $Sr_{0.6}Ba_{0.4}Ce_{0.9}Ga_{0.1}O_{3-\Delta}$ for Proton-Conducting Solid Oxide Fuel Cell Application

Nur Wardah Norman[1], Wan Nor Anasuhah Wan Yusoff[1], Abdullah Abdul Samat[1], Mahendra Rao Somalu[1*], Andanastuti Muchtar[1,2]

[1]Fuel Cell Institute, Universiti Kebangsaan Malaysia, 43600 UKM Bangi, Selangor, Malaysia
[2]Centre for Materials Engineering and Smart Manufacturing (MERCU), Faculty of Engineering and Built Environment, Universiti Kebangsaan Malaysia, 43600 UKM Bangi, Selangor, Malaysia
**Corresponding author E-mail: mahen@ukm.edu.my*

Abstract

$Sr_{0.6}Ba_{0.4}Ce_{0.9}Ga_{0.1}O_{3-\delta}$ (SBCG) electrolyte pellet was prepared by glycine-nitrate method, in which the electrolyte powders and pellets were systematically characterized for their application to proton-conducting solid oxide fuel cells (SOFCs). Thermogravimetric analysis revealed that impurities were formed in the electrolyte powders at the temperature of 1000 °C. X-ray diffraction analysis showed that the powder calcined at 1000 °C produced an electrolyte with high purity. Scanning electron microscopy analysis indicated that the sintered SBCG pellet had a clear morphology and grain boundaries. Therefore, SBCG is a promising electrolyte for SOFC applications.

Keywords: *Proton-conducting electrolyte; solid oxide fuel cell; specific density*

1. Introduction

Solid oxide fuel cells (SOFCs) are electrochemical devices that contain ceramic components and highly depend on oxide ions, and they are operated at temperatures of 800 °C to 1000 °C. This high operating temperature is necessary to enhance the ionic conductivity of ceramic electrolytes during the conversion of chemical energy into electricity through electrochemical reactions driven by the potential difference of the oxygen chemistry between anodes and cathodes. The challenges encountered for this type of fuel cell are the high operating costs and the reliability of the system [1]. The conventional operating temperature of SOFCs lead to stability and reliability problems. Thus, researchers have attempted to decrease the operating temperature from a high (800 °C to 1000 °C) to an intermediate range (400 °C to 700 °C) by developing new electrolyte and electrode materials [2]. Recent studies have shifted toward proton-conducting SOFCs (H^+-SOFCs), which displayed better stability and higher reliability levels than conventional ones at high operating temperatures. H^+-SOFCs can operate at moderate temperatures (< 800 °C) because of the production of water vapor at the cathode during chemical reactions. Consequently, the amount of fuel discharge can be minimized at the anode, resulting in high open circuit voltage values and the ability to control the amount of input fuel [3], [4].

In recent decades, doped $BaZrO_3$, $BaCeO_3$, $SrCeO_3$, and $SrZrO_3$ have been introduced as proton-conducting electrolytes for SOFC applications due to their ability to conduct proton efficiently even at moderate temperatures (< 800 °C). However, these materials are hindered by many challenges, including chemical instability, high grain boundary resistance, and high sintering temperatures [5], [6]. Considering these challenges, researchers have shifted toward developing new and improved proton conducting electrolytes by doping additional small amounts of aliovalent cations, such as Y^{3+} and In^{3+}, and other rare-earth cations, such as Gd^{3+} and Sm^{3+} [7], [8]. The sintered pellet, such as yttrium-doped barium cerate zirconate (BZCY), exhibited a high conductivity at reduced temperature and a good chemical stability under CO_2, H_2O, and H_2S. However, the sinterability of this electrolyte remained low. In the present work, Ga was doped in the B-site of Ce, and Ba was doped in the A-site of Sr to determine the morphology and purity of this new and improved material for H^+-SOFC application [9].

In this work, the $Sr_{0.6}Ba_{0.4}Ce_{0.9}Ga_{0.1}O_{3-\delta}$ (SBCG) powder was synthesized by glycine-nitrate process. The effects of dopants on the structural and morphological characteristics of the materials were investigated by thermogravimetric analysis (TGA), X-ray diffraction (XRD) analysis, and scanning electron microscopy (SEM). The morphology and purity of the synthesized material are critical in evaluating the potentiality of the electrolyte for SOFC application.

Copyright © 2019 Authors. This is an open access article distributed under the Creative Commons Attribution License, which permits unrestricted use, distribution, and reproduction in any medium, provided the original work is properly cited.

2. Materials and method

2.1. Synthesizing the electrolyte powder

The SBCG electrolyte powder was produced by glycine-nitrate process. Strontium nitrate $Sr(NO_3)_2$ and barium nitrate $Ba(NO_3)_2$ were dissolved together, and cerium nitrate $Ce(NO_3)_3 \cdot 6H_2O$ and gallium nitrate $Ga(NO_3)_3 \cdot xH_2O$ were dissolved together in deionized water. Then, the two solutions were mixed and stirred together at room temperature to produce a homogeneous solution mixture. After which, glycine, which serves as a complexing agent and fuel during combustion reactions, was added to the solution [10]. Then, the temperature was raised exponentially to remove the water from the solution until a viscous and visible gel was formed. The heating process was continued until an ignition was triggered to burn the gel and form a fine powder.

2.2. Structural characterization of the electrolyte powder

The electrolyte powder was characterized using TGA and XRD. TGA was conducted starting from 25 °C to 1400 °C at a 10 °C min^{-1} heating/cooling rate through the use of a thermogravimetric instrument, TG (Mettler Toledo, USA). The powder was then calcined at 900 °C, 1000 °C, and 1100 °C for 5 h in a high-temperature furnace (Berkeley Scientific BSK-1700X-S, USA) to remove impurities. Then, the powdered phase structure was processed through the XRD analysis (XRD Bruker D8-Advance, Germany) at the angle of diffraction of 2θ in the range of 20° to 80° with a value of $\lambda = 0.15406$ Å.

2.3. Morphological characterization of electrolyte pellet

For morphological analysis, the electrolyte powder was suppressed into pellets through the process of suppression. For this purpose, 1 g of powder was blended with an agate mortar and placed in a 13 mm diameter pellet mold (Specac PT No. 300, USA). The powder was then pressed at a pressure of 5 tons for 1 min with the use of a hydraulic pressing machine (4350 Carver, USA). The formed pellets were sintered at 1400 °C for 5 h wat a heating/cooling rate of 10 °C min^{-1} in a high-temperature furnace (Berkeley Scientific BSK-1700X-S, USA). The relative density of the pellet was determined by Archimedes' method. The microstructure of the sintered pellets was analyzed using a secondary electron microscope (SEM). The pellets were then broken down and analyzed by scanning electron microscopy (Tabletop Microscope, TM-1000 Hitachi, Japan).

3. Results and discussion

3.1. TG and DT analysis

The TGA of the dried powder are shown in Figure 1. Based on the TG profile and differential thermal analysis, the powder experienced weight loss at three stages for the temperatures ranging from 25 °C to 1400 °C. The observed weight loss at stage 1 (T<480 °C) corresponded to the dehydration of moisture and the decomposition of the remaining organics with low boiling points. The small weight loss that occurred at stage 2 (480 °C to 680 °C) was due to the decomposition of the organic residues to form a carbonate compound [11]. The major weight loss that contributed to the maximum loss recorded at stage 3 resulted from the release/liberation of CO from the carbonate compound [12]. After crossing these three stages, the TG and DT signals started to show horizontal lines, and no further weight loss was recorded. The thermal decomposition analysis indicated that the minimum recommended temperature for the calcination of the SBCG powder was 1000 °C.

3.2. Crystallographic analysis

Figure 2 shows the XRD patterns of the SBCG powders obtained at different calcination temperatures for 5 h. The selective enlargement of the powders can be observed at the diffraction angles of 27°–31°. As shown, the perovskite phase of SBCG was crystallized at the calcination temperature of 1000 °C. However, the XRD profiles showed a weak crystallinity at calcination temperatures above 1000°C because of the partial decomposition of SBCG [13] and the formation of traces of CeO_2 phase [14].

The EDX spectrum verified the presence of Sr, Ba, Ce, and Ga, as presented in Table 1. As shown, the elemental composition in the SBCG compound was close to the actual mole ratio of the elements present in the compound. However, a slight deviation occurred, mainly at the B-site containing element of Ce and Ga, because the analysis was performed only on a number of specific areas that have different elemental distributions [15]. Furthermore, the difference in the amount of mole distribution among the elements was excessively large, which caused Ce to overlap onto Ga. Thus, Ga was difficult to detect in the EDX spectrum, leading to the low chemical composition in terms of the mole ratio [16], [17].

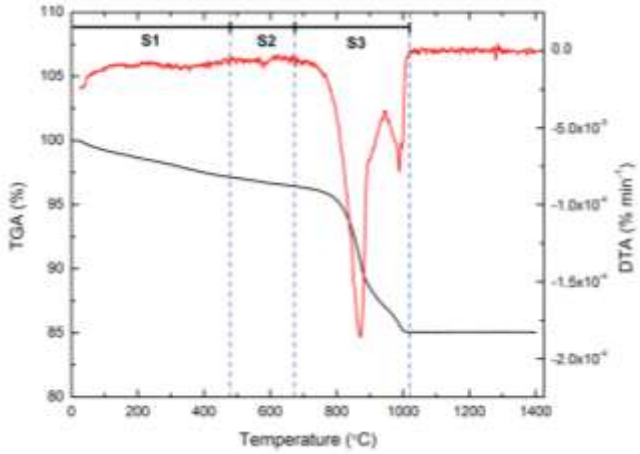


Fig. 1: TG/DTA curves of $Sr_{0.6}Ba_{0.4}Ce_{0.9}Ga_{0.1}O_{3-\delta}$ (SBCG) powders at temperature 25 to 1400 °C

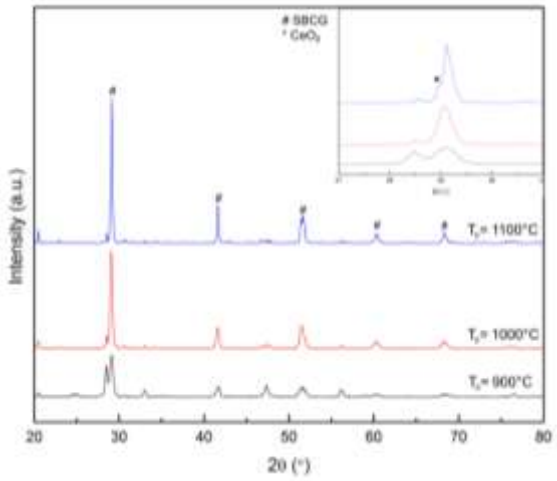


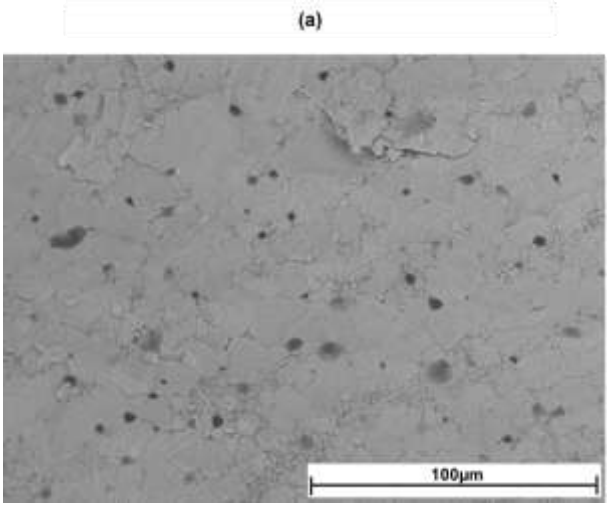
Fig. 2: XRD patterns of $Sr_{0.6}Ba_{0.4}Ce_{0.9}Ga_{0.1}O_{3-\delta}$ (SBCG) powders calcined at 900 °C, 1000 °C, and 1100 °C

Table 1: Elemental composition of $Sr_{0.6}Ba_{0.4}Ce_{0.9}Ga_{0.1}O_{3-\delta}$ (SBCG) powder calcined at 1000 °C for 5 h

Element	Weight %	Relative atomic mass	Mol	Actual mole ratio	Experiment mole ratio
Sr	18.47	87.62	0.21	0.60	0.57
Ba	22.62	137.33	0.16	0.40	0.43
Ce	44.04	140.12	0.31	0.90	0.93
Ga	2.28	114.81	0.02	0.10	0.07

3.3. Morphological characterization

The morphology and grain boundary of the SBCG pellets obtained by SEM analysis are shown in Figure 3. As shown, the sintered pellet of SBCG calcined at 1000 °C had compact, high-density, and well-distributed grains. However, slight porosity was observed at the cross-section of the electrolyte. The specific density of this electrolyte was 99%, which was deemed appropriate for application as a proton conductor. The surface of the pellet indicated that the introduction of new dopants affected the chemical stability and sinterability of the compounds. Larger grain sizes (Figure 3) can offer a less overall grain boundary resistance. Thus, Ga can be added to base materials as a dopant and sintering additive [18].



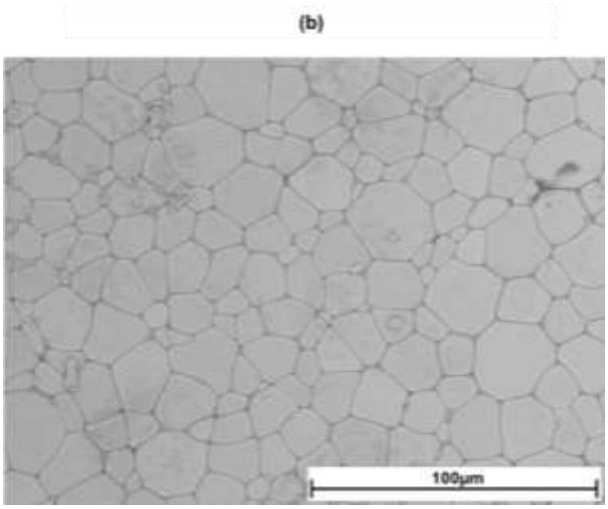


Fig. 3: Micrograph images for (a) cross section and (b) surface of SBCG pellet after sintered at 1400 °C for 5 hours

4. Conclusions

SBCG powder was successfully prepared using the glycine-nitrate process. The properties of the thermal decomposition of the SBCG powder were studied using TGA at a temperature of 1000 °C. The thermal decomposition consisted of three stages, namely, decomposition of water, decomposition of carbon and nitrate compounds, and the formation of carbonate. The SBCG powder sintered at 1400 °C showed compact and uniformly distributed grains with improved density. 1000 °C was determined as the suitable calcination temperature for the electrolyte pellet even though the grain size grew unevenly. The mixing time of the nitrate solution should be increased from 12 to 24 h to enhance the purity of the SBCG powder.

Acknowledgement

The authors would like to thank the Ministry of Higher Education and Universiti Kebangsaan Malaysia for the funding support via the research sponsorship of DIP-2016-005. The Centre for Research and Instrumentation Management (CRIM), UKM and Fuel Cell Institute (ISF), UKM are also acknowledged for excellent preparation and testing facilities.

References

[1] Li M, Ni M, Su F & Xia C (2014), Proton conducting intermediate-temperature solid oxide fuel cells using new perovskite type cathodes. J. Power Sources 260, 197–204.
[2] Rahman HA, Muchtar A, Muhamad N & Abdullah H (2010), Komposit La1-xSrxCo1-yFeyO3-d (LSCF) sebagai bahan katod tahan lama bagi sel fuel oksida pejal bersuhu sederhana-rendah: ulasan kajian. J. Kejuruteraan 22, 1–9.
[3] Singh B, Ghosh S, Aich S & Roy B (2017), Low temperature solid oxide electrolytes (LT-SOE): a review. J. Power Sources 339, 103–135.
[4] Arpornwichanop A, Patcharavorachot Y & Assabumrungrat S (2010), Analysis of a proton-conducting SOFC with direct internal reforming. Chem. Eng. Sci. 65(1), 581–589.
[5] Wang Y, Leung DYC, Xuan J & Wang H (2017), A review on unitized regenerative fuel cell technologies, part B: unitized regenerative alkaline fuel cell, solid oxide fuel cell, and microfluidic fuel cell. Renew. Sustain. Energy Rev. 75, 775–795.
[6] Norby T & Magraso A (2015), On the development of proton ceramic fuel cells based on Ca-doped LaNbO4 as electrolyte. J. Power Sources 282, 28–33.
[7] Liu Y, Guo Y, Ran R & Shao Z (2012), A new neodymium-doped BaZr0.8Y0.2O3−δ as potential electrolyte for proton-conducting solid oxide fuel cells. J. Memb. Sci. 415–416, 391–398.
[8] Radojkovic A, Zunic M, Savic SM, Brankovic G & Brankovic Z (2013), Chemical stability and electrical properties of Nb doped BaCe0.9Y0.1O3-d as a high temperature proton conducting electrolyte for IT-SOFC. Ceram. Int. 39, 307–313.
[9] Yoo Y & Lim N (2013), Performance and stability of proton conducting solid oxide fuel cells based on yttrium-doped barium cerate-zirconate thin-film electrolyte. J. Power Sources 229, 48–57.
[10] Ding X, Ding L, Wang L, Zhu W, Hua G, Liu H, Gao Z & Yuan G (2017), Improved electrochemical activity and stability of LaNi0.6Fe0.4O3-δ cathodes achieved by an in-situ reaction. Electrochim. Acta 236, 378–383.
[11] Osman N, Jani AM & Talib IA (2006), Synthesis of Yb-doped Ba(Ce,Zr)O3 ceramic powders by sol-gel method. Ionics (Kiel). 12, 379–384.
[12] Dahl P, Haugsrud R, Lein H, Grande T, Norby T & Einarsrud MA (2007), Synthesis, densification and electrical properties of strontium cerate ceramics. J. Eur. Ceram. Soc. 27, 4461–4471.
[13] Yuan A, Tian L, Xu W & Wang Y (2010), Al-doped spinel LiAl0.1Mn1.9O4 with improved high-rate cyclability in aqueous electrolyte. J. Power Sources 195(15), 5032–5038.
[14] Lee KR, Tseng CJ, Chang JK, Hung IM, Lin JC & Lee SW (2013), Strontium doping effect on phase homogeneity and conductivity of Ba1−xSrxCe0.6Zr0.2Y0.2O3−δ proton-conducting oxides. Int. J. Hydrogen Energy 38(25), 11097–11103.
[15] Choudhury B & Choudhury A (2013), Oxygen vacancy and dopant concentration dependent magnetic properties of Mn doped TiO2 nanoparticle. Curr. Appl. Phys. 13 (6), 1025–1031.
[16] Samat AA, Somalu MR, Muchtar A & Osman N (2016), Preparation of lanthanum strontium cobalt oxide powder by a modified sol-gel method. Malaysian J. Anal. Sci. 20(6), 1458–1466.
[17] Samat AA, Senari SM, Somalu MR, Muchtar A, Hassan OH & Osman N (2018), Heat treatment effect on the phase and morphology of NiO-BCZY prepared by an evaporation and decomposition of solution and suspension method. Sains Malaysiana 47(3), 589–594.
[18] Hossain S, Abdalla A, Radenahmad N, Zakaria AKM, Zaini JH, Rahman S, Eriksson S, Irvine J & Azad A (2018), Highly dense and chemically stable proton conducting electrolyte sintered at 1200 °C. Int. J. Hydrogen Energy 43(2), 894–907.